Environ Earth Sci (2010) 61:665–674
DOI 10.1007/s12665-009-0378-9

ORIGINAL ARTICLE

Glacial runoff characteristics of the Koxkar Glacier, Tuomuer-Khan Tengri Mountain Ranges, China

Haidong Han · Shiyin Liu · Jian Wang · Qiang Wang · Changwei Xie

Received: 3 March 2009 / Accepted: 17 November 2009 / Published online: 3 December 2009

Abstract This paper presents the glacial runoff characteristics of the Koxkar Glacier, China using flow records collected near the snout of the glacier in four consecutive years (2005–2008). The mean annual discharge of the Koxkar Glacier is 102.86×10^6 m^3, in which 93.6% occurs in ablation season (May–October). August brings about maximum discharge of about 29.6% to the total streamflow followed by July of some 26.0%. During the study years, total discharge varies little from year to year, whereas the inter-annual variability in monthly discharge is prominent, particularly in the beginning and in the end of the melt season. Seasonal runoff variability shows great monthly variations in discharge with mean coefficient of variation ranging from 0.02 in January to 0.77 in April. The mean diurnal amplitudes are found to be 0.90, 1.86, 4.71, 4.92, 1.17 and 0.43 m^3 s^{-1} for May, June, July, August, September and October, respectively. In the melt season, the maximum runoff is observed during 1800–0200 hours and the minimum occurs during 0700–1000 hours. Delaying effects are prominent in discharge over the ablation period. The time-lag between meltwater generation and its appearance in the streamflow near the snout of the glacier varies between 4.00 and 10.00 h, and time to peak varies between 10.00 and 17.00 h over the entire melt season. The relationship between discharge and temperature on monthly scale ($R^2 = 0.77$) is better than that on daily scale ($R^2 = 0.55$).

Keywords Koxkar Glacier · Melt runoff · Diurnal variation · Time-lag · Flow duration

H. Han (✉) · J. Wang
Laboratory of Watershed Hydrology and Applied Ecology in Cold and Arid Regions, CAREERI, Chinese Academy of Sciences, 730000 Lanzhou, China
e-mail: hhd@lzb.ac.cn; leopard1048@126.com

S. Liu · Q. Wang · C. Xie
State Key Laboratory of Cryosphere Science, CAREERI, Chinese Academy of Sciences, 730000 Lanzhou, China

Introduction

Glacier ice presently covers about 10.7% or almost 15.9×10^6 km^2 of the total land area, most of which is contained in the Antarctic (13.6×10^6 km^2) and Greenland (1.7×10^6 km^2). The remaining ice mass (ice caps and alpine glaciers), which represent about only 3.5% ($\sim$550,000 km^2) of the total ice covered area on the Earth's surface, are of great importance for humankind in terms of hydrology because of their active roles in regional and global water circulations (Benn and Evans 1998). In cold season, the glacier melt ceases and most of the precipitation of snow and other forms of ice at the glacier surface was accumulated to the glacier, and in warm season, however, glacier releases a great amount of water to local streamflow and river systems through ablation. The hydrological role of glacier is of special relevance in arid areas like central Asia where meltwater from glacier ice is one of the primary sources of freshwater, and therefore is vital to maintain the functions of the social development of the human being. In terms of northern Tarim River Basin, China, which is one of the most arid regions in Central Asia with annual mean precipitation less than 42.8 mm in the piedmont lowlands (Liu et al. 2006), up to 50–60% of the total river runoff come from melt of snow and glacier ice in the mountain ranges located at the Basin's margin, namely the Tuomuer-Khan Tengri Mountain Ranges (Xie et al. 2004).

The Tuomuer-Khan Tengri Mountain Ranges is the largest glacierized area in Tien Shan Mountains in which a total amount of 629 glaciers were nourished and covered an area of 3,849.47 km^2—2 times greater than that in Qilian Mountain (1,979.8 km^2) and 2.4 times of that in Mount Everest (1,600 km^2) (Su et al. 1985). One of the striking glaciological features of this region is the development of many huge dendritic valley glaciers (also called Tuomuer-type valley glaciers by Chinese glaciologists for their unique characteristics). The center of the Tuomuer-Khan Tengri Mountain Ranges is encircled by six large valley glaciers with areas greater than 100 km^2, out of which the Inylchek is the largest glacier in the Tien Shan Mountains extending over 60 km in length and covering an area of 544 km^2 (Hagg et al. 2008). Another impressive characteristic of these glaciers is their heavy supraglacial debris cover in the ablation areas. The data compiled in Chinese Glacier Inventory (Tien Shan Mountains Volume) show that more than 60% of the ablation area of a Tuomuer-type valley glacier is covered by supraglacial debris. The extensive supraglacial debris entrainment, on the one hand, modifies surface energy balance and prevents glacier from rapid wastage; and on the other hand, affects glacial runoff generation and streamflow regime (Han et al. 2006; Xie et al. 2007).

Now the Tarim River Basin is under increasing pressure on freshwater demand due to population growth, farmland expansion and industrial development (Zhou et al. 2003). Hydrological investigations of alpine glaciers at the Basin's margin become necessitous because of their importance in terms of irrigation, drinking water supply, hydroelectric power generation and regulating of water use policies. In effect, a number of state or regional hydrological gauging sites have been established on the main rivers in this area since 1950s, to record the hydrological variability of the rivers at multi-temporal scales (Gao and Wang 2008). All of these gauging sites, however, have been set up in the piedmont plain and far away from glaciers in high altitudes, which implies that the glacial runoff variability captured by these gauge sites has been greatly interfered by streamflow originated from non-glacierized areas, and thus presents a different hydrological regime compared with that measured near the glacier snout due to differences in runoff generation, water storage, drainage characteristics and water compensation effect (Ferguson 1985; Röthlisberger and Lang 1987; Singh and Singh 2001).

In the last 30 years, a number of glaciers in Tuomuer-Khan Tengri Mountain Ranges have been subject to short-term investigations (usually during specific project duration) on mass balance, glacial meteorology and glacial hydrology (Liu et al. 2006). As the foremost requirement to reveal the hydrological characteristics of any glacier is the continuous and reliable flow data for several years, our understanding on the regime of the glacial runoff is still limited in this region due to absence of long-term hydro data. Recently, a four-year-long (2005–2008) flow data of the Koxkar Glacier, Tuomuer-Khan Tengri Mountain Ranges, has been derived through successive field investigations. These data provide a good opportunity to further understand the runoff characteristics of the glaciers in this region. The purpose of the present work is to understand the glacial runoff characteristics of a Tuomuer-type glacier, including season distribution of streamflow, runoff variability on annual and seasonal scales, diurnal runoff variations, runoff delaying characteristics, runoff-temperature relationship and flow-duration curves.

Study site

Koxkar Glacier (41°42N–41°53N and 79°59E–80°10E) (Fig. 1) is a typical Tuomuer-type glacier (Su et al. 1985) originating from Mt. Koxkar (6,342 m a.s.l.), and flows southeast to the terminus of 3,020 m a.s.l. The glacier extends 25.1 km in length and covers an area of 83.56 km^2. The equilibrium line occurs at 4,300 m a.s.l. in the icefall from whose foot a 15.5-km-long, debris-mantled glacier tongue appears. The supraglacial debris covers an area of about 19.5 km^2, which accounts for 83% of the total ablation area, with thicknesses ranging from less than 0.01 m on the upper reach of the ablation area and on ice-cliff faces to more than 3.0 m near the glacier snout (Han et al. 2006). The altitudinal distribution of glacierized and not-glacierized area of Koxkar Glacier basin is shown in Fig. 2.

Two glacial runoff outlets exist on the Koxkar Glacier (Fig. 1): the main outlet lies in the glacier terminus from which most of the meltwater flows out of the glacier, and the other outlet locates at the western side of the glacier tongue, where a very little proportion (less than 1%) of meltwater escapes from the ice body and flows westward to feed the vicinal village. Due to small quantity of water flow and its little influence upon the total glacial runoff, the melt runoff flowing out of the western exit has not been observed, and the discharge and meteorological observations were only conducted in the gauging sites near the glacier terminus since 2005.

Date collection

The hydrological gauging site was established about 800 m downstream of the snout of glacier, in which the minimal requirements for a hydrological gauging site were meet, such as flow of water in a single channel, straight river

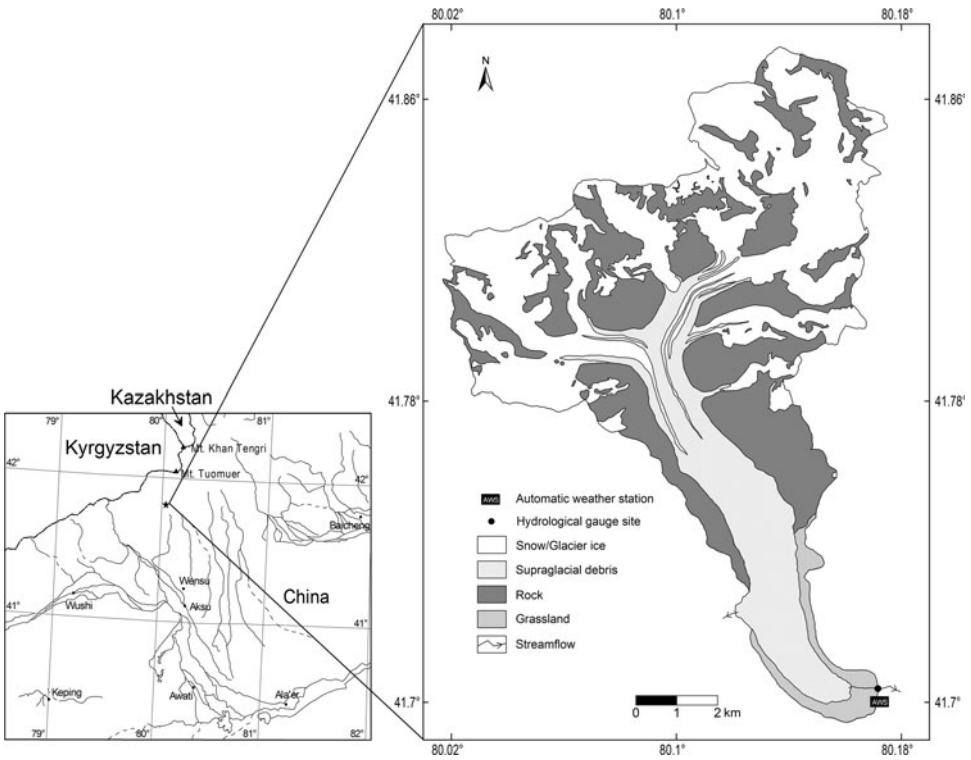

Fig. 1 Location of Koxkar Glacier, Tuomuer-Khan Tengri Mountain Ranges, China

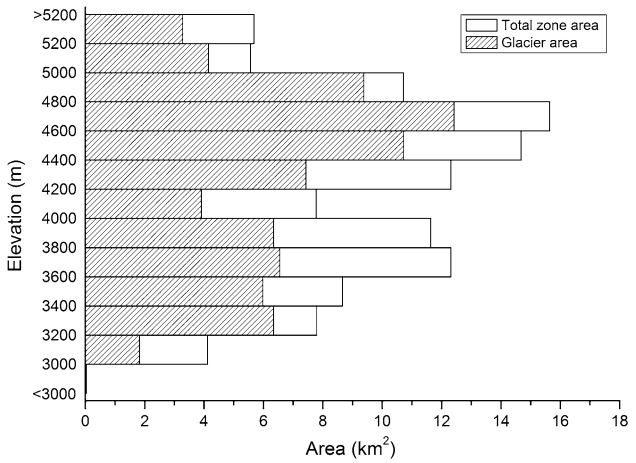

Fig. 2 The altitudinal distribution of glacierized and not-glacierized area of Koxkar Glacier basin

course with length long enough and minimal turbulence in flow, etc. A stilling well was constructed on the right bank of the river, and an automatic barometric sensor (HOBO Water Level Logger, Onset Computer Corp.) was installed in the well to record hourly variations in bulk pressure (water and atmospheric pressure). A graduated staff gauge was installed near the stilling well for manual observations of water level and to provide a reference when converts bulk pressure into water level. A simple bridge was built across the river channel to facilitate the measurement of flow velocity using propeller blade current meter (Model LS25-1, Huazheng Hydrometric Instrument Ltd). The river channel was divided into six to nine segments (depends on the channel width in different season) and flow velocity was measured at each place. Coupled with mean flow velocity and cross-section area of each segments, channel discharge at specific water level can be obtained. After measures of discharge at a range of water level, particularly maximum and minimum water level in a year, a stage–discharge relationship was developed for each measurement years (2005–2008).

An automatic weather station (AWS) was established on the grassland about 100 m southward to the hydrological gauging site. The elevation of the AWS is 3,009 m a.s.l. There are many sensors mounted on the AWS monitoring a range of environmental variables, out of which three meteorological sensors are most relevant to this study, i.e. air temperature and relative humidity probe (HMP45C, Campbell Scientific Inc., mounted at 2 m above ground surface), wind sensor (05103 wind monitor, R.M. Young Company, mounted at 2 m above ground surface), and barometric pressure sensor (PTB210, Campbell Scientific Inc., installed at 1 m above ground surface). The sensors were connected to a datalogger (CR1000, Campbell Scientific Inc.) which provides hourly records for each variable.

In order to retrieve continuous water level from bulk pressure measurement, a statistical relationship between stage and water pressure (bulk pressure minus atmospheric pressure) must be established, and then with the help of the

stage–discharge relationship, time series of flow discharge can be calculated from retrieved water level. In terms of the Koxkar Glacier, the discharge data covering four consecutive years (2005–2008) has been successfully derived. A range of factors can reduce the precision of flow data, including high flow velocity variability from warm to cold season, uneven river bed and errors in water level measurement. Taking all these factors into account, the possibility of errors in flow measurements is in the range of ±8%.

Results and discussion

Seasonal distribution of streamflow

Previous works concerning runoff division based on water component analysis (Xie 2006) indicates that melting of ice and snow from the Koxkar Glacier are the main sources of proglacial streamflow. Rain-induced water flow accounts for about 6.8% of the total glacial runoff, and thus being neglected in the streamflow distribution analysis.

With the help of stage–discharge relationship, the continued water level measurement at the established gauging site provides hourly flow data for all the study years. These hourly flow data were used to calculate the daily mean flow at the gauging site. Figure 3a presents the variations of daily mean streamflow for 2005 through 2008, and Fig. 3b demonstrates the monthly distribution of discharges for corresponding years. It is observed that, in cold seasons (November–April), the streamflow maintains at a low level, and the streamflow in these periods is primarily supplied by groundwater (>90%) (Xie 2006) and water of glacial sources including ice melting under thick debris layer, en- and sub-glacial ablation and release of glacier storage. From May onward the discharge starts increasing, reaching its peak in August, and then starts reducing. Table 1 gives the mean monthly discharge and water yield from January to December using collected flow records for all the study years. It shows that annual mean discharge of the proglacial stream of the Koxkar Glacier is 102.86×10^6 m^3, out of which 93.6% occurs in ablation season (May–October). Specifically, August contributes about 29.6% to the total streamflow followed by July of some 26.0%. In terms of streamflow in ablation season, August and July receive about 59.3% of the total melt runoff. This value is most close to that observed in Gangotri Glacier (56.4%), central Himalayas (Singh et al. 2006), and is lower than that derived in Austre Brøgrerbreen (80%), Arctic region (Hodgkins 1997) where the ablation season is much shorter.

Glacial runoff variability

Interannual variability

The total glacial runoff is estimated to be 103.02, 102.36, 102.23 and 103.83×10^6 m^3 for 2005, 2006, 2007 and 2008, respectively. Results show that during the study years, there is little variation in total runoff from year to year. To better understand the interannual variability of the glacial runoff, the variation in monthly discharge from year to year is calculated using monthly flow data of all the study years (Fig. 4). The coefficient of variation

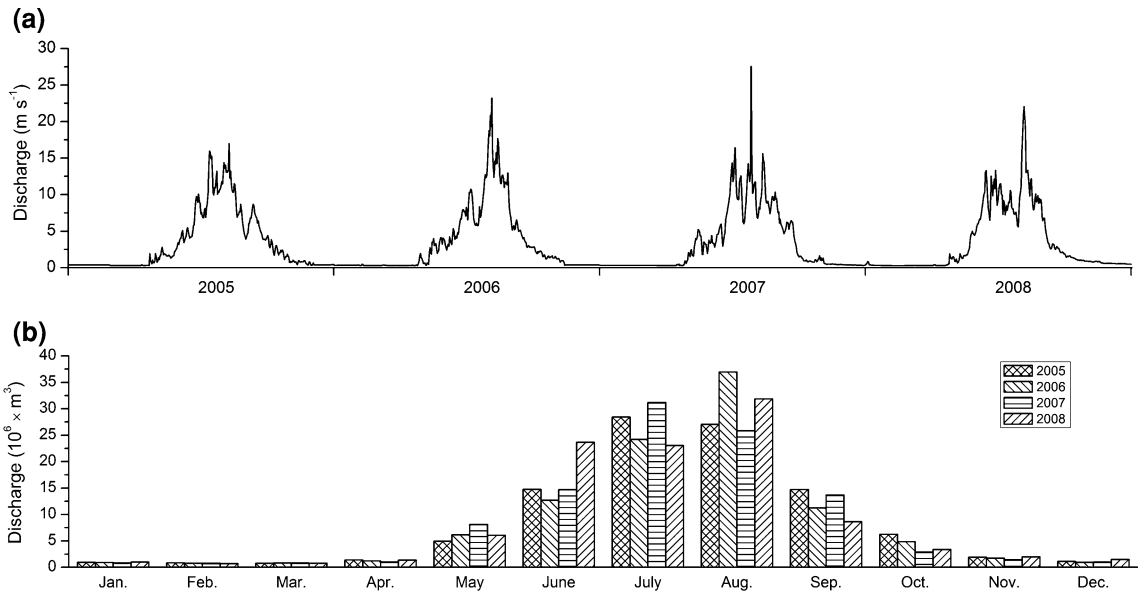

Fig. 3 **a** Daily mean discharge and **b** monthly discharge observed during consecutive study years

Table 1 Mean monthly discharge and water yield computed using 4 years data on Koxkar Glacier

	Jan	Feb	Mar	Apr	May	June	July	Aug	Sep	Oct	Nov	Dec
Discharge (m s^{-1})	0.34	0.32	0.3	0.48	2.36	6.34	9.97	11.36	4.65	1.62	0.67	0.42
Discharge ($\times 10^6$ m^3)	0.92	0.77	0.80	1.23	6.32	16.44	26.70	30.42	12.06	4.33	1.75	1.12
Water yield (mm)	7.87	6.59	6.84	10.52	54.06	140.62	228.38	260.20	103.16	37.04	14.97	9.58

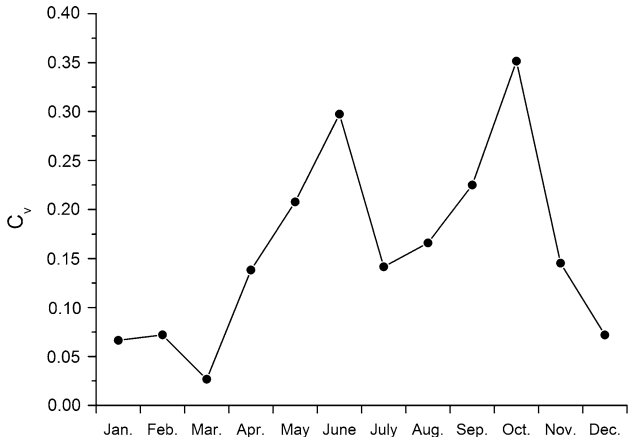

Fig. 4 Interannual variability of monthly discharge reflected by coefficient of variation (C_v)

(C_v, defined as the ratio of standard deviation to the mean) is adopted here to quantified the discharge variability. Figure 4 shows that runoff variation in January, February, March and December is very limited year by year, indicating a stable outflow from the glacier in cold season. Nevertheless, discharge in May, June, September and October exhibit high interannual variability, which may be related with the large interannual variation in synoptic systems in the period of seasonal transition, i.e. from the cold season to the warm and vice versa. In July and August, the coefficient of variation, C_v, are around 0.15, which denoting small interannual variation in these months.

Seasonal variability

Since solar radiation and air temperature are dominating factors controlling melting of ice and snow, the melt runoff varies with these meteorological forcing, and thus displays distinct monthly variability. To be comparable, the monthly variation of runoff as well as temperature was calculated for the four study years, using daily flow data and corresponding air temperature records of each month (Fig. 5). The coefficient of variation, C_v, is reapplied in this analysis to describe the variability of runoff and temperature and to compare the both. Because applying C_v to the time series involving samples with negative value may yield wrong results, i.e. negative C_v, $C_v > 1$ or overflow

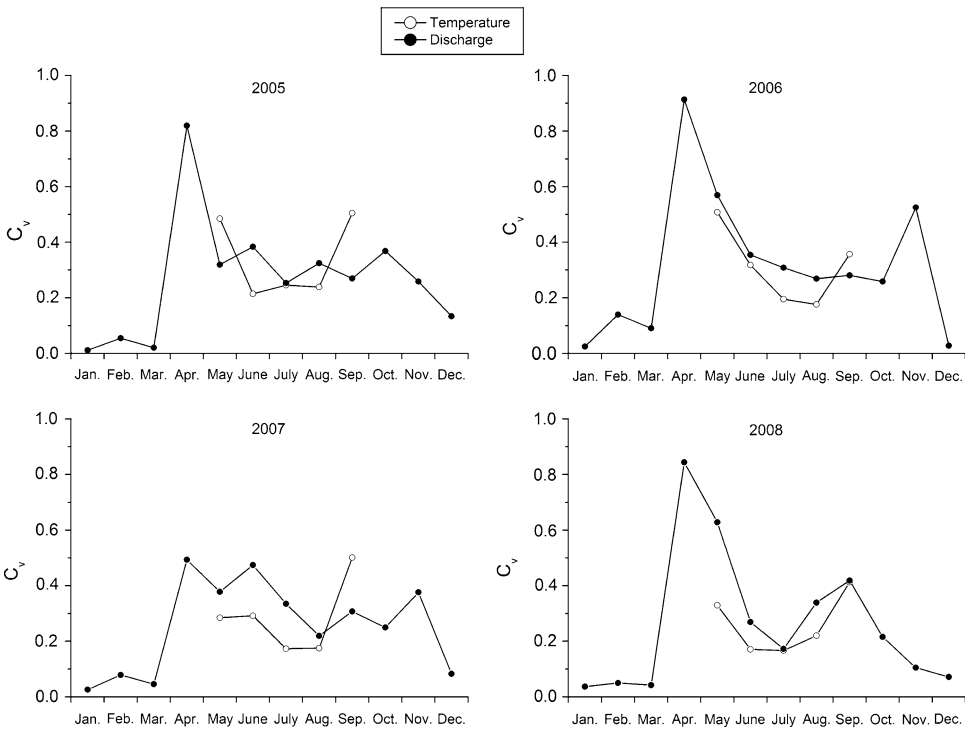

Fig. 5 Changes in coefficient of variation (C_v) for discharge and temperature over the year

error when the mean is zero (Faber and Korn 1991), the temperature variability in cold season is not presented, and only results of May, June, July, August and September, in which the daily mean temperatures are positive, are given in Fig. 5. The absence of temperature variability in months from November to March, however, has less influence on the discussion of seasonal variability in streamflow since, during that period, the temperature is very low and the supraglacial ablation ceases, and thus the variation of glacial runoff is practically independent of temperature. In case of April and October, details are given below.

Results presented in Fig. 5 illustrate great monthly variations in discharge with mean coefficient of variation ranging from 0.02 in January to 0.77 in April. The maximum discharge variability found in April may be due to fast increase in discharge induced by intense melting of seasonal snow at the end of the month, as compared to low flow in the beginning and mid of the month. From May to September, the variability in runoff and temperature displays similar pattern: dropdown gradually from May to August and then start increasing. The second maximum occurs in the end of the melt season, and its position varies among September, October and November, depending on the temperature variations, glacier storage behavior, precipitation availability and other factors in the corresponding months. During the whole winter (December to the next March), the discharge variability usually maintains at a low level due to stable ground water supply to the streamflow.

Diurnal variations of discharge

Figure 6 depicts mean diurnal variations in discharge computed for different months in ablation period using 4 years data. It shows that the diurnal variability in runoff is positively related with discharge. During the early and the later part of the melt season, the discharge is small and the daily hydrograph is almost flat. With advancement of melt season, the discharge increases with well-distinguished diurnal variability. It is suggested that the seasonal shift of the diurnal discharge variation results from seasonal cycle of weather systems as well as variations in physical features in glacierized basin with time. This result is consistent with works carried out on the Gangotri Glacier, Himalayas (Singh et al. 2006) with modified backgrounds in climate conditions and glacier characteristics. At the beginning of the melt season (May–June), the temperature is relatively low and a large extent of winter snow exists, particularly in the upper reaches of the ablation zone. As such, runoff of melting snow and ice is less and part of which is intercepted by snowpack, supraglacial ponds, englacial conduits, etc. as glacier storage before it flows out of the snout of the glacier. Therefore, the discharge observed near the terminus is less with small diurnal

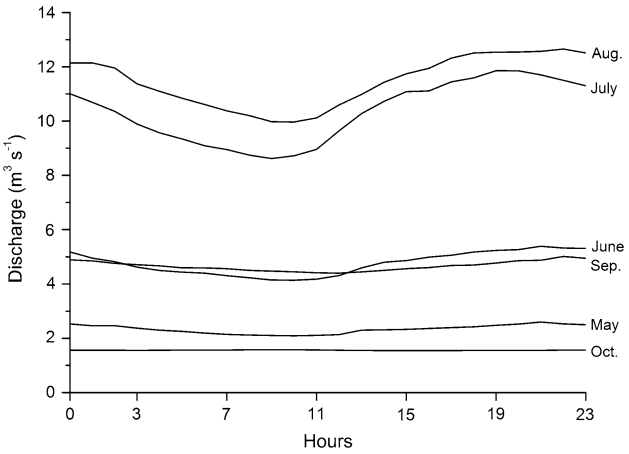

Fig. 6 Mean diurnal variations in discharge computed for different months in ablation period using 4 years data

amplitudes at this stage. The pronounced diurnal variability in discharge in the mid of the ablation season (July–August) is primarily related with (i) large extent of exposed ice which makes intense melting to be possible under high temperature background, (ii) larger temperature variations on diurnal scale with higher mean temperature, which leads to large difference in ablation rate between daytime and nighttime and (iii) minimum snow extent and developed drainage network which minimize the influences of glacier storage on the melting runoff and make the discharge to be more responsive to the diurnal forcing. At the end of the ablation season (September–October), the diurnal pattern of discharge generally duplicates that at the beginning of the melt season except for more even hydrographs. This result may be attributed to the release of the precedent meltwater that stored in the glacier. During the period with cold temperature (November–April), however, the diurnal variations in discharge is substantially free of meteorological controls because the main component of the streamflow comes from ground water instead of snow/ice melting, and thus flat daily hydrographs are expected for months at this stage.

Calculations on the diurnal runoff amplitudes from daily hydrographs show that, during the melt season for all the study years, the mean diurnal amplitudes are 0.90, 1.86, 4.71, 4.92, 1.17 and 0.43 $m^3 s^{-1}$ for May, June, July, August, September and October, respectively, with runoff amplitude ratio (defined as the diurnal runoff amplitude expressed as a proportion of the diurnal mean flow) to be 0.37, 0.40, 0.46, 0.43, 0.25 and 0.24 for corresponding months.

Delay characteristics of discharge

Figure 6 also reveals that the maximum runoff is observed during 1800–0200 hours and the minimum occurs during

0700–1000 hours. The timing of maximum and minimum flow varies with season depending on the changes in meteorological conditions, altitudinal distribution of snow and ice and glacier drainage network. This fact is further related with two variables that characterizing the delaying effect in glacial runoff variation, i.e. time to peak (t_{peak}) and time-lag (t_{lag}) between meltwater generation and its appearance in the streamflow near the snout of the glacier. As solar radiation directly influences the snow/ice melting, the commonly adopted criteria for time-lag analyses is that hydrograph should be of clear weather day, which brings maximum insolation and higher temperature. In the case study, however, the employment of traditional procedure is problematic because the overall clear weather days are rare in the melt season due to strong local circulation (Han et al. 2008). A typical "good weather" day in the melt season of Koxkar Glacier is that it is clear in the morning and evening and overcast or raining in the afternoon, which leads to large fluctuation in occurrence of maximum of air temperature (T_{max}) (ranging from 1,200 to 1,800), and subsequently, influences the timing of maximum discharge (Q_{max}). To compute mean monthly time-lag and time to peak values, 5 days were selected from each month in melt season, 2007, on the basis of (i) maximum solar radiation and higher temperature allowing intense snow/ice melt to happen, (ii) free of rainfall in that day as well as in its former and next days to exclude rain-induced cases and (iii) evenly distributed in the month to present representative mean monthly results. Since year to year variations in mean t_{lag} and t_{peak} for corresponding months are not significant, the case study for months in 2007 is thought to be representative to present delaying characteristics in charge on Koxkar Glacier.

As shown in Table 2, t_{lag} is calculated as the time-lag between T_{max} and Q_{max}, and t_{peak} is the time consumption from minimum discharge (Q_{min}) to the maximum (Q_{max}). It is observed that both t_{lag} and t_{peak} are higher in the early and end of the ablation season as compared to the peak melt season. t_{lag} varied between 4.00 and 10.00 h, and t_{peak} varied between 10.00 and 17.00 h over the entire melt season. Monthly mean time-lag are 8.00, 6.60, 5.40, 5.20, 8.00 and 8.80 h for May, June, July, August, September and October, respectively, and mean time to peak are 15.00, 14.80, 12.40, 13.00, 13.60 and 14.80 h for corresponding months. In terms of glacier physics, the magnitude of runoff delay depends on the distance the meltwater has to travel through and below the glacier, and the configuration of internal drainage network (Benn and Evans 1998). In the beginning of the melt season, underdeveloped internal drainage networks, such as narrow drainage passages and linked-cavity networks, and strong glacier storage due to presence of large extent of seasonal snow cover lead to significant delaying effects on melt runoff transportation. As the melt season progresses, the seasonal snow shrinks to higher altitudes and has less storage implications for melt runoff, and the drainage system of the glacier becomes more efficient when carrying large discharges (Seaberg et al. 1988; Hock and Hooke 1993). Thus, both t_{lag} and t_{peak} are reduced during this period. Toward the end of the melt season, t_{lag} and t_{peak} are higher, which may be associated with melt runoff reducing and snow cover extending. The former factor is related with inefficiency of drainage network in water transportation (Jansson et al. 2003), and the latter is related with significant storage effect on melt runoff.

Delaying characteristics of discharge in months of cold season are not discussed in the proposed paper because, during that period, melt runoff is very few and discharge and temperature are actually not interrelated.

Glacier runoff-temperature relationship in melt season

The melting of ice and snow is primarily controlled by the energy available for melt, which is linked to air temperature. Therefore, examining of the relationship between glacial runoff and air temperature provides a quick and rough tool to evaluate the quantity and variations of the melt runoff for a glacierized basin. Figure 7a, b presents the scatter maps of mean monthly and mean daily melt depth versus corresponding air temperatures, considering data in melt season of all the study years. It shows that the variations in discharge have not been fully captured by temperature records. The low correlation between discharge and temperature may be due to significant influences of non-melting-induced events and progresses in discharge, for example rain-caused cases, runoff delaying and glacier storage effects. Even this, the trends in discharge and temperature variations are coincident both on monthly and daily scales. Generally, the relationship between mean monthly depth of discharge and mean monthly temperatures ($R^2 = 0.77$) is better than that between mean daily runoff depth and mean daily temperatures ($R^2 = 0.55$). The better relationship between discharge and temperature on monthly scale may be due to the reduction in variability of both discharge and temperature on monthly scale (C_v for discharge = 0.64, C_v for temperature = 0.50) when compared with daily scale (C_v for discharge = 0.72, C_v for temperature = 0.60).

Flow-duration curve

The flow-duration curve provides information about the percentage of time that a particular streamflow is equaled or exceeded over some historical period, and it has long been used as means of summarizing catchment hydrologic response (Cole et al. 2003). Figure 8a, b presents the flow-

Table 2 Timing of T_{max}, Q_{max}, Q_{min}, time-lag and time to peak for May–October, 2007 on Koxkar Glacier

Month	Time of T_{max} (hours)	Time of Q_{max} (hours)	Time of Q_{min} (hours)	Time-lag t_{lag} (h)	Time to peak t_{peak} (h)
May	02/05 1700	03/05 0200	02/05 0900	9.00	17.00
	09/05 1200	09/05 2100	09/05 0700	9.00	14.00
	15/05 1700	16/05 0000	15/05 0800	7.00	16.00
	22/05 1700	23/05 0000	22/05 0800	7.00	16.00
	28/05 1200	28/05 2000	28/05 0800	8.00	12.00
June	02/06 1500	02/06 2300	02/06 0800	8.00	15.00
	09/06 1700	09/06 2300	09/06 0800	6.00	15.00
	15/06 1700	15/06 2300	15/06 0900	6.00	14.00
	19/06 1700	20/06 0000	19/06 0900	7.00	15.00
	29/06 1700	29/06 2300	29/06 0800	6.00	15.00
July	04/07 1500	04/07 2000	04/07 0800	5.00	12.00
	11/07 1700	11/07 2100	11/07 0700	4.00	14.00
	18/07 1600	18/07 2200	18/07 0700	6.00	15.00
	24/07 1200	24/07 1800	24/07 0700	6.00	11.00
	28/07 1200	28/07 1800	24/07 0800	6.00	10.00
August	05/08 1700	05/08 2100	05/08 0900	4.00	12.00
	13/08 1800	13/08 2200	13/08 0700	4.00	15.00
	17/08 1400	17/08 2000	17/08 0900	6.00	11.00
	21/08 1600	21/08 2100	21/08 1000	5.00	11.00
	28/08 1700	29/08 0000	28/08 0800	7.00	16.00
September	02/09 1200	02/09 1900	02/09 0700	7.00	12.00
	08/09 1400	08/09 2200	08/09 0900	8.00	13.00
	15/09 1500	15/09 2200	15/09 0800	7.00	14.00
	19/09 1600	20/09 0200	19/09 0900	10.00	17.00
	27/09 1200	27/09 2000	27/09 0800	8.00	12.00
October	03/10 1300	03/10 2200	03/10 0700	9.00	15.00
	10/10 1500	10/10 2300	10/10 0800	8.00	15.00
	15/10 1400	15/10 2100	15/10 0800	7.00	13.00
	19/10 1300	19/10 2300	19/10 0800	10.00	15.00
	25/10 1400	26/10 0000	25/10 0800	10.00	16.00

duration curves over the entire season and the melt season, respectively, using daily flow data for the four consecutive years (2005–2008). The discharge corresponding to 25, 50, 75 and 90 percentage of time is found to be 5.08, 0.95, 0.33 and 0.29 $m^3\ s^{-1}$ for the entire season, and 8.90, 5.02, 2.28 and 1.35 for the melt season, respectively. Flat curves observed near the upper limits on both curves exhibit the typical characteristic of the glacierized river, whereas the straight curve in the lower proportion on Fig. 8a indicates the low base flow sustained throughout the year. To better understand the characteristics of amplitude and frequency in monthly discharge over the melt season, monthly flow-duration curves for May through October were plotted in Fig. 9 using daily flow records from 2005 to 2008. It shows that, during the melt season, the flow-duration curves for each month are much flatter and moderate flows are found in the upper limits for most of the curves, which indicates temperate variations in amplitudes of melt runoff in ablation period. This fact may be attributed to continued water supply from snow/ice melt to the streamflow and significant glacier regulations upon the melt runoff through glacier storage and drainage network. The only steep curve observed in the upper proportion of the flow-duration curve in July is supposed to be related with the flood events of supraglacial lake outburst. Dozens of supraglacial lakes or ponds are distributed in the debris-covered area of Koxkar Glacier. The outburst of these lakes or ponds may be triggered by the interactions of lakes to englacial drainage passageways by ice ablation and/or water calving (Ageta et al. 2000). Therefore, the risks of supraglacial lake outburst increase in July and August when ice ablation is intense. The outburst of the large supraglacial lakes,

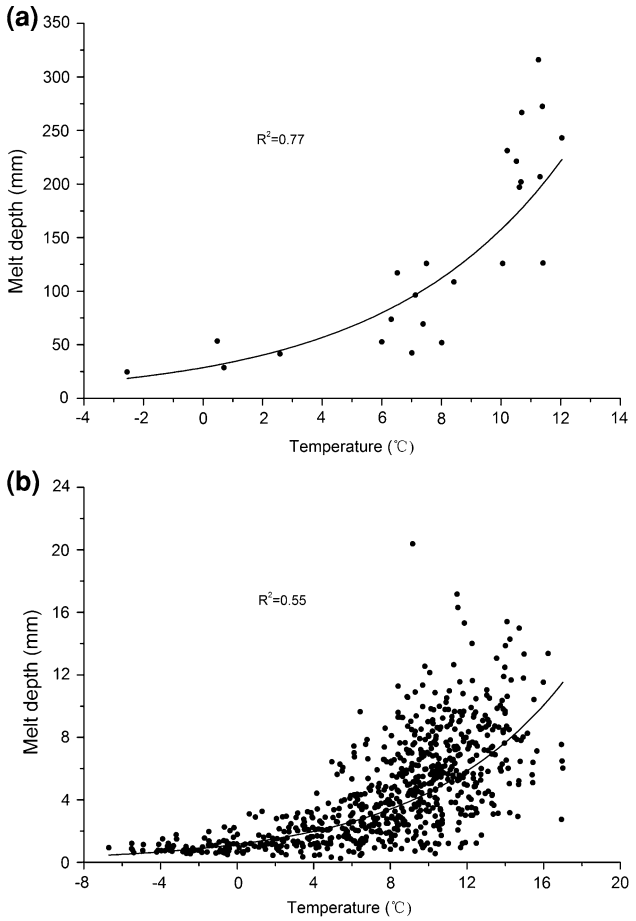

Fig. 7 Relationship between **a** mean monthly melt depth and mean monthly air temperatures, and **b** mean daily melt depth and mean daily air temperatures considering data in melt season of all the study years

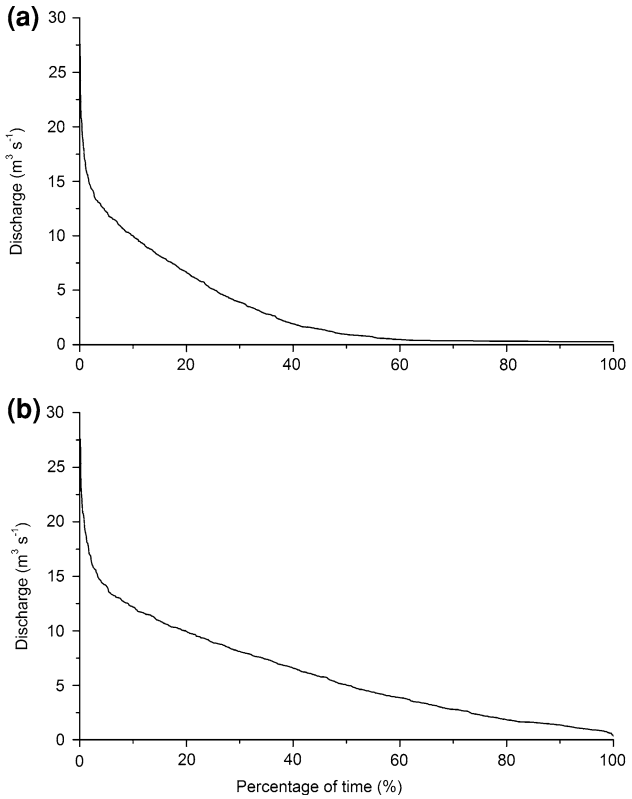

Fig. 8 Flow-duration curves for **a** the entire season and **b** the melt season developed using daily flow records collected near the snout of the Koxkar Glacier

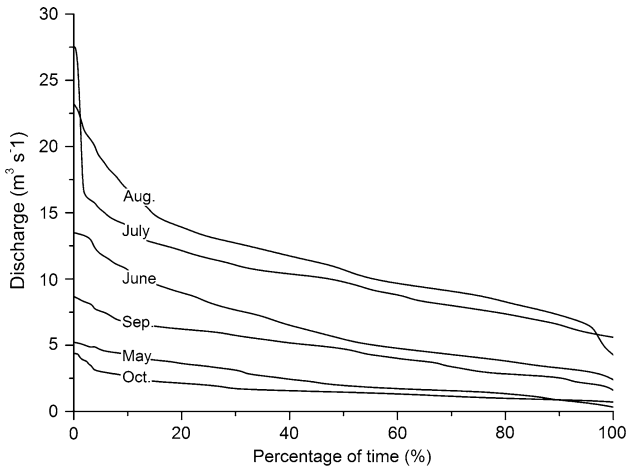

Fig. 9 Flow-duration curves for different months in the melt season using daily discharge observed near the snout of the Koxkar Glacier

however, is not frequent according to the field investigations, and thus has less influence on the overall pattern of the flow-duration curves.

Conclusions

Hydrological analysis on the proglacial streamflow is one of the major works in modern glacier investigations. The proposed paper investigates the hydrological characteristics of Koxkar Glacier, China using flow data observed near the snout of the glacier for four consecutive years. The study reveals that annual mean discharge of the proglacial stream of the Koxkar Glacier is to be 102.86×10^6 m^3, out of which 93.6% occurs in melt season (May–October). The maximum contribution to the total flow is from August (29.6%) followed by July (26.0%). The interannual runoff variability for months displays lower coefficient of variations when compared with seasonal variability, and the maximum occurs in June and October. The diurnal variability in runoff is positively related with discharge. During the early and later part of the melt season, the discharge is small and the flow curve is almost flat. With advancement of melt season, the discharge increases with well distinguished diurnal variability. At the end of the ablation season, the diurnal pattern of discharge duplicates that at the beginning of the melt season except for more

even hydrograph. The mean diurnal amplitudes are 0.90, 1.86, 4.71, 4.92, 1.17 and 0.43 $m^3 s^{-1}$ for May, June, July, August, September and October, respectively. On the basis of daily hydrograph, time-lag and time to peak are calculated to present delaying characteristics of the melt runoff. The results show that monthly mean time-lag are 8.00, 6.60, 5.40, 5.20, 8.00 and 8.80 for May, June, July, August, September and October, respectively, and mean time to peak are 15.00, 14.80, 12.40, 13.00, 13.60 and 14.80 h for corresponding months. The flatter curves are observed in the upper limit of flow-duration curves, which is typical characteristic of a glacierized basin. The steep upper proportion observed in the flow-duration curve for July indicates occasional runoff contribution from supraglacial lake outburst flood to the main streamflow.

The results present in this paper are preliminary towards fully understanding of the glacial runoff characteristics on Koxkar Glacier because a range of important issues have not been addressed due to absence of relevant data. These issues include long-term variations in discharge in the scenario of climate warming, influence of rain on the discharge, characteristics of the internal drainage system, sediment transportation in streamflow, etc. The field observations concerning these issues are ongoing or under preparation.

Acknowledgments This work was supported by the Nation Basic Research Program of China (973 Program) under grant No. 2007CB411501, National Nature Science Foundation of China (NSFC) program under grant No. 40601020, National Basic S&T Project of the Ministry of Science and Technology of the People's Republic of China under grant No.2006FY110200, Knowledge Innovation Program of the Chinese Academy of Sciences under grant No. KZCX2-YW-301, and China International Science and Technology Cooperation Program under grant No. 2008DFA20400. The authors thank Wang Shunde, Xu Jindong and Jiang Li for their kindly supports on the field investigations and data collection. We appreciate Professor P. Singh and his works for giving us great inspirations and encouragements to accomplish this study.

References

Ageta Y, Iwata S, Yabuki H, Naito N, Sakai A, Narama C, Karma (2000) Expansion of glacier lakes in recent decades in the Bhutan Himalayas. In: Nakawo M, Raymond CF, Fountain A (eds) Debris covered Glaciers. IAHS pub. no.264, pp 165–175

Benn DI, Evans DJA (1998) Glaciers & glaciation. Wiley, New York, p 716

Cole RAJ, Johnston HT, Robinson DJ (2003) The use of flow duration curves as a data quality tool. Hydrol Sci J 48(6):939–951

Faber DS, Korn H (1991) Applicability of the coefficient of variation method for analyzing synaptic plasticity. Biophys J 60(5):1288–1294

Ferguson RI (1985) Runoff from glacierized basins: a model for annual variation and its forecasting. Water Resour Res 21:702–708

Gao QZ, Wang R (2008) Impact of climate change on surface runoff of Tarim River originating from the south slopes of the Tianshan Mountains (in Chinese with English abstract). J Glaciol Geocryol 30(1):1–11

Hagg W, Mayer C, Lambrecht A, Helm A (2008) Sub-debris melt rates on southern Inylchek Glacier, central Tian Shan. Geogr Ann Series A Phys Geogr 90(1):55–63

Han HD, Ding YJ, Liu SY (2006) A simple model to estimate ice ablation under a thick debris layer. J Glaciol 52(179):528–536

Han HD, Liu SY, Ding YJ, Deng XF, Wang Q, Xie CW, Wang J, Zhang Y, Li J, Shangguan DH, Zhang PF, Zhao JD, Niu L, Chen CP (2008) Near-surface meteorological characteristics on the Koxkar Baxi Glacier, Tianshan (in Chinese with English abstract). J Glaciol Geocryol 30(6):967–975

Hock R, Hooke RL (1993) Evolution of the internal drainage system in the lower part of the ablation area of Storglaciären, Sweden. Geol Soc Am Bull 105(4):537–546

Hodgkins R (1997) Glacier hydrology in Svalbard, Norwegian high Arctic. Quat Sci Rev 16(9):957–973

Jansson P, Hock R, Schneider T (2003) The concept of glacier storage: a review. J Hydrol 282(1–4):116–129

Liu SY, Ding YJ, Zhang Y, Shangguan DH, Li J, Han HD, Wang J, Xie CW (2006) Impact of the glacial change on water resources in the Tarim River Basin (in Chinese with English abstract). Acta Geogr Sin 61(5):482–490

Röthlisberger H, Lang H (1987) Glacial hydrology. In: Gurnell AM, Clark MJ (eds) Glacio-fluvial sediment transfer. Wiley, New York, pp 207–284

Seaberg SZ, Seaberg JZ, Hooke RL, Wiberg DW (1988) Character of the englacial and subglacial drainage system in the lower part of the ablation area of Storglaciären, Sweden, as revealed by dye-trace studies. J Glaciol 34(117):217–227

Singh P, Singh VP (2001) Snow and glacier hydrology. Kluwer, The Netherlands, p 742

Singh P, Haritashya UK, Kumar N, Singh Y (2006) Hydrological characteristics of the Gangotri Glacier, central Himalayas, India. J Hydrol 327(1–2):55–67

Su Z, Song GP, Wang LL, Zhang WJ, Zhang HY, Yang CT, Liang D (1985) Glaciers and weather in Mt. Tuomuer District (in Chinese). Xinjiang Peoples Publishing House, Urumqi, p 224

Xie CW (2006) Analysis and modeling of hydrological characteristics on Koxkar Glacier, south slop of Mt. Tuomuer (in Chinese). PhD Dissertation, p 147

Xie CW, Ding YJ, Liu SY, Han HD (2004) Analysis on the glacial hydrological features of the glaciers on the south slope of Mt. Tuomuer and the effects on runoff (in Chinese with English abstract). Arid Land Geogr 27(4):570–575

Xie CW, Ding YJ, Chen CP, Han TD (2007) Study on the change of Keqikaer Glacier during the last 30 years, Mt. Tuomuer, Western China. Environ Geol 51(7):1165–1170

Zhou YZ, Pan XL, Wang FY (2003) Basic problems on the Tarim River water resources reallocation project in short term. Proc SPIE 4890:400–405